Chapter 8

High-Porosity Metal Foams: Potentials, Applications, and Formulations

Ahmed Niameh Mehdy Alhusseny, Adel Nasser and Nabeel M J Al-zurfi

Additional information is available at the end of the chapter

http://dx.doi.org/10.5772/intechopen.70451

Abstract

This chapter is aimed as a concise review, but well-focused on the potentials of what is known as "High-porosity metal foams," and hence, the practical applications where such promising media have been/can be employed successfully, particularly in the field of managing, recovering, dissipating, or enhancing heat transfer. Furthermore, an extensive comparison is conducted between the formulations presented so far for the geometrical and thermal characteristics concerning the heat and fluid flow in open-cell metal foams.

Keywords: high porosity, open cell, metal foam, fluid flow, thermal transport

1. Introduction

A porous medium can be defined as a material composed of a solid matrix consisting of interconnected voids. This solid matrix is usually assumed to be rigid, but sometimes it may undergo limited deformations. The interconnected pores allow for a single type of fluid or more to flow through the material. There are many examples of these permeable materials available in nature such as sand beds, limestone, sponges, wood, and so on.

Porous media have become one of the most important materials used in insulating, transferring, storing, and dissipating thermal energy. The benefits these characteristics confer have led to porous materials being widely used in practical applications such as thermal insulation, geothermal applications, cooling systems, recuperative/regenerative heat exchangers, and solar energy collection systems, in addition to chemical and nuclear engineering. Thus, convective flows in porous materials have been investigated widely over recent decades and various aspects have been considered for different applications so far.

High-porosity metal foams are usually porous media with low density and novel structural and thermal properties. This sort of media is mainly formed from multi-struts interconnected to each other at joint nodes to shape pores and cells (see the SEM image in **Figure 1**) (Liu et al. [1]). They offer very high porosity ($\varepsilon \geq 0.89$), light weight, high rigidity and strength, and a large surface area, which make them able to recycle energy efficiently. This capacity to transport a large amount of heat is attributed to their superior thermal conductivity compared to ordinary fluids and high surface-area density (surface area per a given volume of metal foam) as well as enhanced convective transport (flow mixing) due to the tortuous flow paths existing within them, as shown in **Figure 1** (Zhao [2]). Also, their open-cell structure makes them even less resistant to the fluids flowing through them, and hence, the pressure drop across them is much less than it is in the case of fluid flow via packed beds or granular porous materials.

Open-cell metal foams were first invented by the ERG Materials and Aerospace Corp. in 1967, and since then, they have been continuously developed. This invention was patented to Walz [3], where the manufacturing processes were based on an organic preformation cast. However, this invention was originally intended for only classified military and aerospace applications. Accordingly, nonclassified applications had not made use of this technology until the mid of 1990s, when it has become generally available for industrial applications. Since then, other manufacturers have joined the global competition in this industry. To name a few, M-Pore GmbH in Germany, the French company Alveotec, and Constellium from Netherlands are currently making open-cell metal foams on a large scale for a wide range of applications.

The traditional way of casting open-cell metal foams is still adopted by ERG Materials and Aerospace [4] as well as M-Pore GmbH [5], where the foams are cast with an investment process based on polyurethane preformation. As the fabrication process is affected by gravity, the foams resulted will be shaped from oval rather than spherical cells, as illustrated in **Figure 2** (De Schampheleire et al. [6]). Alveotec [7] and Constellium, on the other hand, use a different way called leachable bed casting, in which metal is cast over a stack of soluble spheres to shape out the interconnecting open-cells desired. The spheres used are usually made out of either salt

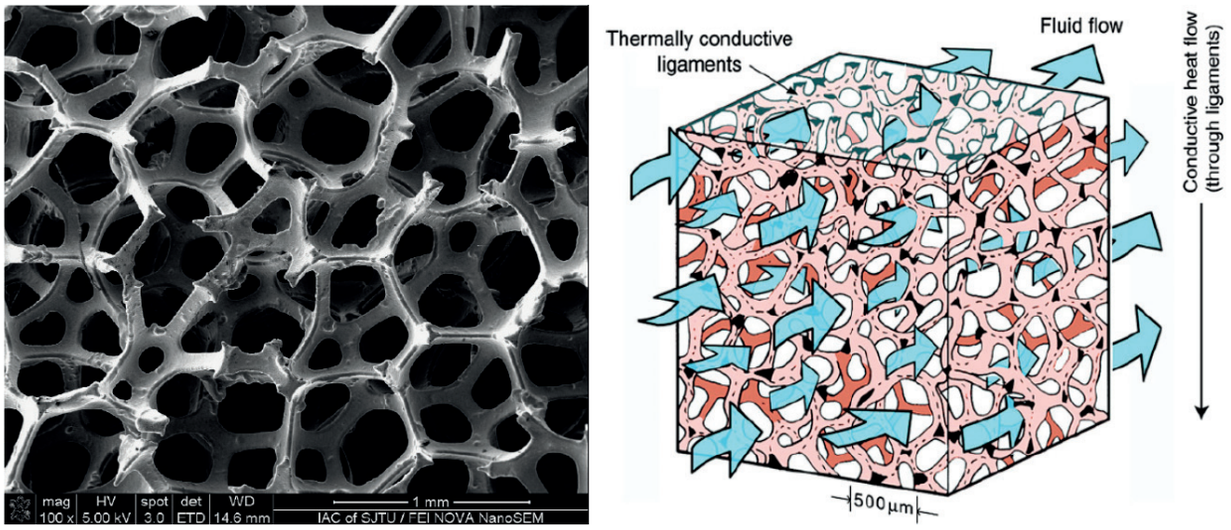

Figure 1. Open-cell metal foams: SEM image of the structure (left); mechanism of flow mixing (right).

http://dx.doi.org/10.5772/intechopen.70451

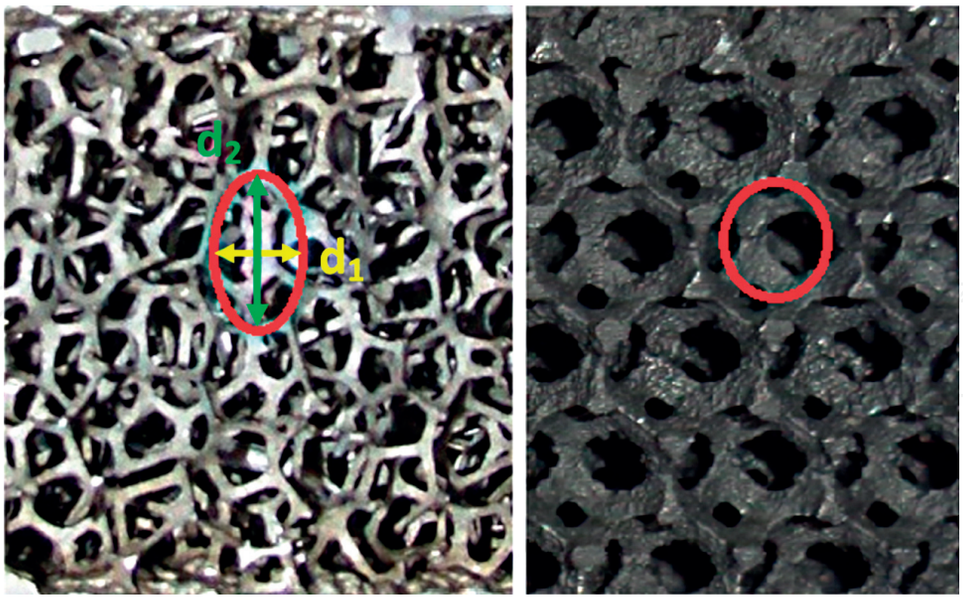

Figure 2. Open-cell metal foams formed by: Investment casting (left); (b) leachable bed casting (right).

or sand plus a polymer bonding agent. After metal solidification, the spheres are dissolved through washing them simply with water. Using this casting technique results in foams having more uniformly spherical-shaped cells unlike those formed by the investment casting, as shown in **Figure 2** (De Schampheleire et al. [6]).

2. Potentials

Open-cell metal foams possess unique characteristics, making them a promising candidate for plenty of practical and engineering applications. Among these potentials are the following:

1. Very high porosity, ranges usually from 80% and up to 97.5%.
2. The open-core structure makes them attractive for applications where lightweight is a crucial requirement.
3. The open-cell nature makes them even less resistant to the fluids flowing through them, resulting in a significant saving in the pressure drop resulted.
4. Very high effective thermal conductivity.
5. High surface-area density, roughly from 1000 to 3000 m^2/m^3. Therefore, exceptional heat transfer area per a given volume of metal foam is offered. The surface area density can be further increased through compressing them in a particular direction, where the specific surface area of such a compressed metal foam can reach up to 8000 m^2/m^3 [2].
6. The tortuous flow paths existing within them considerably enhance the convective transport (flow mixing).
7. They are efficient sound-absorption materials [8].

8. They have the potential to be used for radiation shielding [9].
9. Good-impact energy absorption [10], where the structure of metal foam makes it possible to ensure a constant stress throughout the deformation.
10. Have attractive stiffness/strength properties and can be processed in large quantity at low cost via the metal sintering route.

3. Applications

Due to their uniquely promising potentials, high-porosity metal foams have been increasingly utilized in a variety of engineering and industrial applications. Such applications are diversely increasing day by day, making it quite hard to categorize them into particular groups. Thus, it is aimed herein to present an overview of their most recent applications without intensely going into details.

Their ability to meet the increasing daily demands to effectively transfer, exchange, or dissipate heat has attracted researchers and manufacturers to utilize them as a successful alternative to traditional heat transport media. For example, the experiments conducted by Boomsma et al. [11] showed that the thermal performance offered by the compressed open-cell aluminum foam heat exchangers is usually two to three times higher than that achieved through the commercially available heat exchangers, while they require comparable pumping power. Similarly, Mahjoob and Vafai [12] pointed out that despite the potential increase in pressure loss, utilizing metal foams in heat exchangers leads to a substantial enhancement in heat transfer, which can compensate the increase in pressure drop.

Therefore, metal foam heat exchangers have emerged recently in various practical sectors. Among them, metal foams were used as alternative to find extended surfaces utilized in removing heat from geothermal power plants, where metal foam heat exchangers offer superior thermal performance compared to conventional finned surfaces, at no extra cost resulting from the pressure drop and/or material weight [13]. In this regard, wrapping a thin layer of foam around the surfaces of tubes was proposed to enhance the heat transferred from/to them with little increase in the pressure drop produced [14–16]. Despite the higher pressure loss resulted from the increase in foam layer thickness, it was observed that the exterior convective resistance is reduced significantly, and hence, a considerable transfer enhancement is achieved. Also, the overall performance attained through using the foam-covered tubes was comparable to that achieved by the helically finned tubes at the low levels of inlet velocities and far superior at the higher velocities.

In the context of HVAC&R applications, metal foams have been presented as a promising candidate to replace the conventionally finned heat exchangers. Dai et al. [17] compared the heat transfer performance of a flat-tube, louvered-fin heat exchanger with that obtained using an identical foam heat exchanger. The analytical results revealed that for the same fan power and heat transfer performance, the metal foam heat exchanger is significantly more economical in both size and weight for a wide range of design requirements. In another comparison study

[18], it was observed that the heat transfer rate offered by metal-foam heat exchangers is up to six times better than that in the case of the bare-tube bundle with no extra fan power. Also, it was found that if the dimensions of the foamed heat exchanger are not fixed, that is, the frontal area can be manipulated, metal-foam heat exchangers outperform the louvered-fin heat exchanger. In other words, a smaller metal-foam heat exchanger can be used for the same thermal duty, and hence, a smaller fan can perform what is required.

Employing high-porosity metal foams to improve the thermal effectiveness of counterflow double-pipe heat exchangers has been the subject of increasing interest recently. Xu et al. [19] pointed out that to achieve high thermal effectiveness, that is, greater than 0.8, porosity and pore density should be in the range of ($\varepsilon < 0.9$) and ($\omega > 10$ PPI), respectively. Furthermore, Chen et al. [20] observed that despite the increase occurred in the pressure drop, using metal foams results in a remarkable heat transfer enhancement (by as much as 11 times), which leads to a considerable improvement in the comprehensive performance, that is, up to 700%. More recently, an innovative double-pipe heat exchanger was proposed [21, 22] through using rotating metal foam guiding vanes fixed obliquely to force fluid particles to flow over the conducting surface while rotation. Furthermore, the conducting surface itself was covered with a metal foam layer to improve the heat conductance across it. To optimize the performance achieved, an overall performance system factor, that is, *OSP*, was introduced as the ratio of the heat exchanged to the total pumping power required. Overall, the negligibly small pumping power required compared to the amount of heat exchanged makes the overall performance of such heat exchangers incomparable, that is, $OSP = O(10^2)$ (**Figure 3**) (Alhusseny et al. [22]). It was also observed that while increasing the temperature difference from 30 to 300°C, the overall performance achieved can be improved up to 200–300% depending on the *Re** value. This outcome indicates the promising prospects to utilize the proposed configuration as a recuperator in gas turbine systems.

Now, utilizing metal foam can offer as more as twice the cooling effectiveness obtained by the traditional finned heat exchangers. Thus, such a sort of heat exchangers is widely employed today in medical and medicinal products, defense systems, industrial power generation plants,

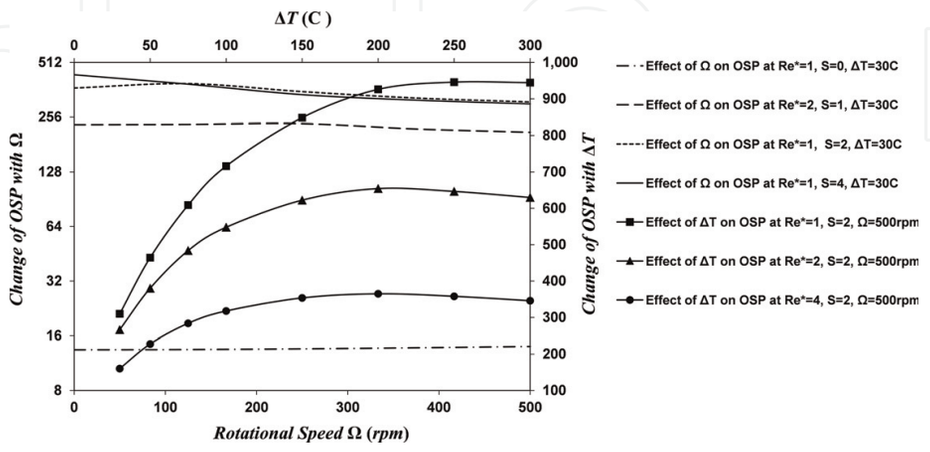

Figure 3. The change of the overall system performance *OSP* with the rotational speed Ω and characteristic temperature difference ΔT for $\varepsilon = 0.9$ and $\omega = 10$ PPI.

semiconductor, manufacturing, and aerospace manned flight [4]. Similarly, they have been proposed as an effective way to enhance the heat dissipated from heavy-duty electrical generators through filling their rotating cooling passages either fully or partially with open-cell metal foams [23–25]. The value of the this proposal was inspected by introducing an enhancement factor as the ratio of heat transported to the pumping power required, that is, $\frac{Nu}{Re\left(p_{in}-p_e\right)/\rho u_{in}^2}$, and comparing it with the corresponding values from a previous work regarding turbulent flow in a rotating clear channel [26], as shown in **Figure 4** [25], where it was confirmed that the proposed enhancement is practically justified and efficient.

They have also been utilized effectively in electronic cooling, where various configurations of metal foam heat sinks have been suggested [27–33] as an effective alternative to the traditional heat sinks incorporated in electronic devices.

In similar context, utilizing metal foams to improve internal cooling of turbine blades is of increasing interest. Filling a radially rotating serpentine channel with open-cell aluminum foam is proposed as an effective way to improve the overall efficiency of the cooling process [34]. Recently, heat transport enhancement along a 180°. round channel was proposed through placing multiple aluminum foam blocks alternately along the flow path [35]. It was found that using discrete foam blocks increases the heat transported by 74–140% compared to what the empty channel yields. In addition, it was observed that staggering the foam blocks vertically is more desirable for improving the overall system performance.

Due to their capability to transport heat effectively, metal foams are shaped into rings placed between the combustor and the turbine section of a jet engine in order to homogenize the temperature profiles of the gases leaving the combustor and, hence, to improve the overall efficiency of turbojet engines [36]. To provide a stable isothermalized platform for the airborne laser communication systems, ERG Materials & Aerospace [4] have fabricated aluminum foam

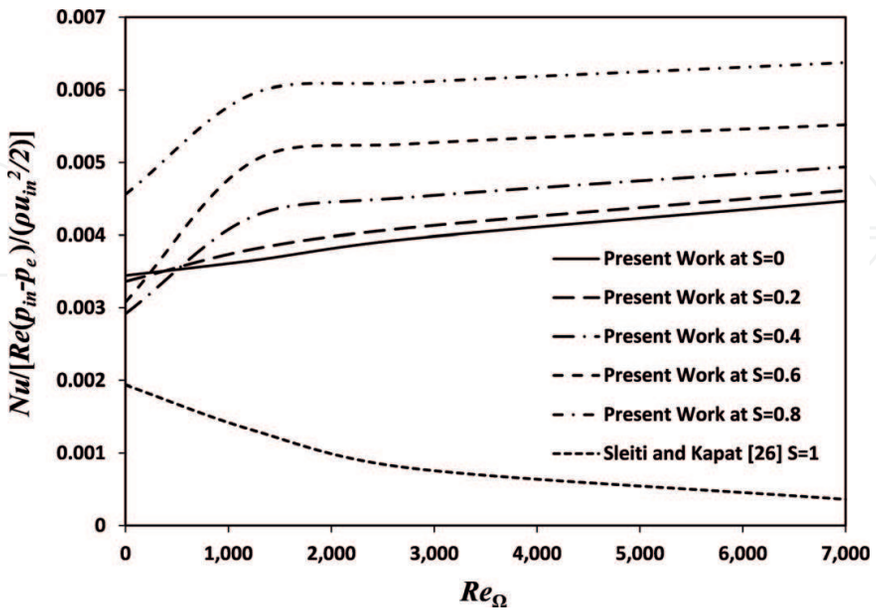

Figure 4. Influence of ΔT on the overall system performance; at $S = 2$, $\Omega = 500$ rpm, and $T_{c1} = 20°C$.

composite opticals having the ability to allow unprecedented heat transfer. In the experiments conducted by Williams et al. [37], a porous insert material (PIM) formed of high porosity foam was proposed to improve the swirl stabilization in LPM combustion systems. It was found that using a reticulated foam insert results in mitigating the thermoacoustic instability effectively as well as reducing the combustion noise over the entire frequency range for a wide range of the design parameters considered.

As most of the phase change materials (PCMs) used for latent heat thermal energy storage (LHTES) possess poor thermal conductivity, the charging/discharging rate achieved will be quite modest. To overcome this deficit, high porosity metal foams have been suggested by Zhao et al. [38] as an effective means to improve the PCMs' overall thermal conductivity, leading to enhance the heat transported and, hence, promote the PCM melting and solidification, as can be seen in **Figure 5** (Alhusseny et al. [39]). This concept has been extensively investigated later to further improve the performance achieved, to name a few, the works presented for low-temperature [40–42] and high-temperature LHTES systems [43–45].

Open-cell aluminum foams are considered as promising lightweight materials for γ-ray and thermal neutron shielding materials. The data collected experimentally by Xu et al. [46] reveal that filling the foam with water results in improving the mass attenuation coefficients compared to the nonfilled samples. Overall, following such a proposal to achieve high shielding performance is still in progress [47, 48] and requires further optimizations.

Overall, there is a variety of applications where high-porosity metal foam can be utilized successfully. For further applications, ERG Materials & Aerospace [4] lists diverse sorts of applications whether in daily life or military industries. For example, open-cell metal

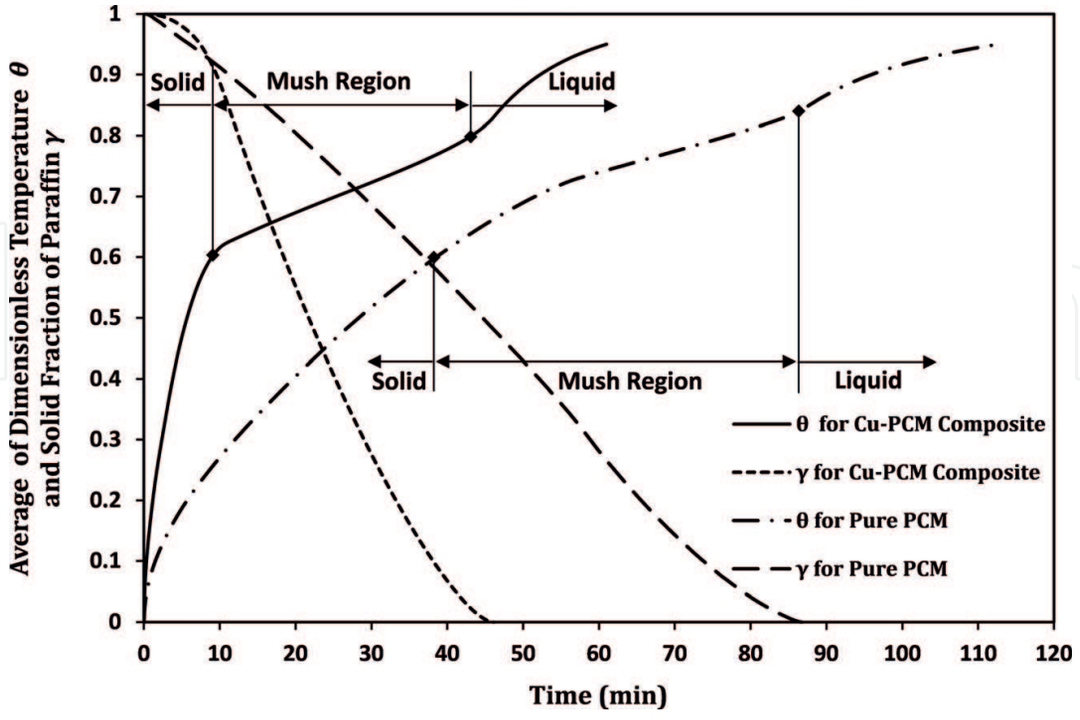

Figure 5. Time development of charging process of paraffin-copper foam composite vs. pure paraffin.

foams are commonly used as energy absorber in aerospace and military applications, air/oil separators in aircraft engine gearboxes, baffles to prevent sudden surges in liquids while being penetrated by solid frames, and breather plugs in applications requiring fast equalization of pressure changes. Also, they are utilized in electrodes, fuel cells, bone researches, micrometeorite shields, optics/mirrors, windscreens and so on. Manufacturers' data and the open literature can be further dug for much more applications where high-porosity metal foams have outperformed and/or achieved considerable savings in the expenses required.

4. Formulations

Open-cell metal foams are classified as high-porosity materials that consist of irregularly shaped and tortuous flow passages. Pressure drop and heat transfer through such media are significantly affected by their geometrical characteristics, namely the foam porosity ε, fiber size d_f, pore diameter d_p, pore density ω, and cell shape. Therefore, most aspects regarding granular porous media and packed beds need to be adjusted for metal foams [11].

4.1. Estimation of fiber and pore diameter

In practice, the ligament size, or in other words fiber diameter, is usually measured using a microscope. Alternatively, the mean pore diameter can be estimated by counting the number of pores that exist in a particular length of foam, which is usually provided by the manufacturer in terms of pore density (PPI), that is, number of pores per inch. Depending on the representative unit cell used (**Figure 6**), various models were proposed. Among them is the model proposed by Fourie and Du Plessis [49] for pore size estimation as a function of the width of a cubic representative unit cell and tortuosity (Eq. (1)). Another model was developed by Calmidi [50] to estimate the fiber- to pore-diameter ratio as a function of the porosity and shape function, $G = 1 - e^{-(1 - \varepsilon)/0.04}$, for both the cubic unit cell (Eq. (2)) and the three-dimensional structure of a dodecahedron unit cell (Eq. (3)).

Fourie and Du Plessis [49]:

$$d_p = d\frac{2}{(3-\chi)}, \quad d = d_p + d_f \tag{1}$$

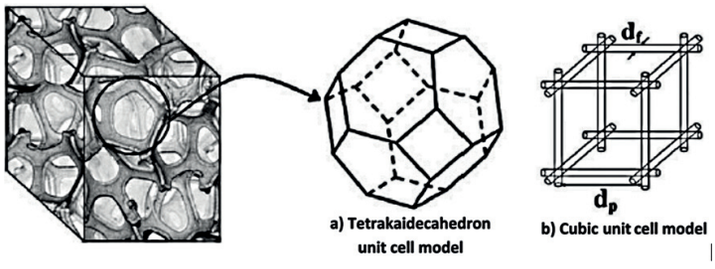

Figure 6. Models used to represent microstructural unit cells in metal foams.

Calmidi [50]:

$$\frac{d_f}{d_p} = 2\sqrt{\frac{(1-\varepsilon)}{3\pi}}\frac{1}{G} \tag{2}$$

$$\frac{d_f}{d_p} = 1.18\sqrt{\frac{(1-\varepsilon)}{3\pi}}\frac{1}{G} \tag{3}$$

4.2. Models developed for predicting tortuosity of high-porosity metal foams

The tortuosity, defined as the total tortuous pore length within a linear length scale divided by the linear length scale in the porous medium [49], was modeled by Du Plessis et al. [51] as a function of porosity only (Eq. (4)). However, experiments conducted by Bhattacharya et al. [52] indicated that the accuracy of tortuosity model proposed by Du Plessis et al. [51] is limited for higher levels of pore density; hence, a tortuosity formulation that accurately covers a wider range of porosity and pore densities was established in terms of porosity and shape function G (Eq. (5)). Recently, an analytical model was proposed by Yang et al. [53] (Eq. (6)), as a simple function of both foam porosity and a pore shape factor. The shape factor β is defined as the ratio of the representative pore perimeter to the perimeter of a typical reference circle with an area equal to that of the representative pore.

Du Plessis et al. [51]:

$$\frac{1}{\chi} = \frac{3}{4\varepsilon} + \frac{\sqrt{9-8\varepsilon}}{2\varepsilon}\cos\left\{\frac{4\pi}{3} + \frac{1}{3}\cos^{-1}\left[\frac{8\varepsilon^2 - 36\varepsilon + 27}{(9-8\varepsilon)^{3/2}}\right]\right\} \tag{4}$$

Bhattacharya et al. [52]:

$$\frac{1}{\chi} = \frac{\pi}{4\varepsilon}\left\{1 - \left(1.18\sqrt{\frac{(1-\varepsilon)}{3\pi}}\frac{1}{G}\right)^2\right\} \tag{5}$$

Yang et al. [53]:

$$\chi = \frac{\beta\varepsilon}{1-(1-\varepsilon)^{1/3}} \tag{6}$$

4.3. Models developed for estimating pressure drop across open-cell metal foams

With regard to predicting the pressure drop produced in fluid flows across high-porosity metal foams, a variety of models have been developed, which can be classified into two main categories. The first encompasses those investigations interested in estimating the pressure drop by means of the foam friction factor. Among them is the model presented by Paek et al. [54] for the friction factor as a function of pore Reynolds number (Eq. (7)). Also, the empirical correlations established by Liu et al. [55] offer friction factor estimation for airflow via aluminum foams for a wide range of porosity and various flow regimes (Eq. (8)).

Paek et al. [54]:

$$f = \frac{1}{\mathrm{Re}_K} + 0.105 \quad f = \frac{(\Delta P/L)\sqrt{K}}{\rho u^2}, \ \ and \ \ \mathrm{Re}_K = \frac{\rho u \sqrt{K}}{\mu} \tag{7}$$

Liu et al. [55]:

$$\left.\begin{array}{l} 30 < \mathrm{Re}_{D_P} < 300 : f = \dfrac{22(1-\varepsilon)}{\mathrm{Re}_{D_P}} + 0.22 \\ \mathrm{Re}_{D_P} >> 300 : \quad f = 0.22 \end{array}\right\} \tag{8}$$

$$f = \frac{(\Delta P/L) D_P}{\rho u^2} \frac{\varepsilon^3}{1-\varepsilon}, \ \ and \ \ \mathrm{Re}_{D_P} = \frac{\rho u \sqrt{K}}{\mu}$$

The other category of pressure drop models consists of those concerned with estimating the permeability and inertial coefficient according to Darcy–-Forchheimer's equation:

$$\frac{dp}{dx} = \frac{\mu}{K} u + \frac{\rho F}{\sqrt{K}} u^2 \tag{9}$$

Based on a cubic representative unit cell, a theoretical model for predicting permeability and inertial coefficient was derived by Du Plessis et al. [51] (Eqs. (10) and (11)), as functions of porosity, tortuosity, and the width of cubic representative unit cell. In the study conducted by Calmidi [50], mathematical models were developed for both permeability and inertial coefficient as functions of the fiber and pore diameters as well as the foam porosity (Eqs. (12) and (13)). A correlation was established by Bhattacharya et al. [52] for predicting the inertial coefficient (Eq. (14)), in terms of tortuosity, porosity, shape function, and form drag coefficient $C_D(\varepsilon)$. Based on Ergun's law $\left(\frac{\Delta p}{L} = \alpha \frac{(1-\varepsilon)^2}{\varepsilon^3 d^2} \mu u + \beta \frac{(1-\varepsilon)}{\varepsilon^3 d} \rho u^2\right)$, Tadrist et al. [56] developed an empirical model for estimating permeability and inertial coefficient as functions of foam porosity and fiber size (Eqs. (15) and (16)). In the experiments conducted by Dukhan [57], the pressure drop resulting from airflow across aluminum foam was correlated into a model predicting the permeability and inertial coefficient as functions of porosity only (Eqs. (17) and (18)). Recently, an analytical model for estimating the permeability of metal foams (Eq. (19)) was established by Yang et al. [53] according to the cubic representative unit cell. This model offers the capability of estimating the permeability for a wide range of foam porosities ε = 0.55 ~ 0.98 and pore densities ω = 5 ~ 100 PPI.

Du Plessis et al. [51]:

$$K = \frac{\varepsilon^2 d^2}{36\chi(\chi - 1)} \tag{10}$$

$$F = \frac{2.05\chi(\chi - 1)}{\varepsilon^2(3 - \chi)} \frac{\sqrt{K}}{d} \tag{11}$$

Calmidi [50]:

$$K = 0.00073 d_p^2 (1-\varepsilon)^{-0.224} \left(\frac{d_f}{d_p}\right)^{-1.11} \tag{12}$$

$$F = 0.00212 (1-\varepsilon)^{-0.132} \left(\frac{d_f}{d_p}\right)^{-1.63} \tag{13}$$

Bhattacharya et al. [52]:

$$\left.\begin{aligned} F &= 0.095 \frac{C_{D(\varepsilon=0.85)}}{12} G^{0.2} \sqrt{\frac{\varepsilon}{3(\chi-1)}} \left(1.18 \sqrt{\frac{(1-\varepsilon)}{3\pi}} \frac{1}{G}\right)^{-1} \\ &0.85 < \varepsilon < 0.97: \quad G = 1 - e^{-(1-\varepsilon)/0.04} \\ &\varepsilon \geq 0.97: \quad G = 0.5831 \end{aligned}\right\}, \ \textit{and}, \ C_{D(\varepsilon=0.85)} = 1.2 \tag{14}$$

Tadrist et al. [56]:

$$K = \frac{\varepsilon^3 d_f^2}{\alpha (1-\varepsilon)^2}, \quad \alpha : 100 \sim 865 \tag{15}$$

$$F = \frac{\beta (1-\varepsilon)}{\varepsilon^3} \frac{\sqrt{K}}{d_f}, \quad \beta : 0.65 \sim 2.6 \tag{16}$$

Dukhan [57]:

$$K = a_1 e^{b_1 \varepsilon} \tag{17}$$

$$F = (a_2 \varepsilon + b_2) \sqrt{K} \tag{18}$$

a_1, a_2, b_1, and b_2 are all constants

Yang et al. [53]:

$$\frac{K}{d^2} = \frac{\varepsilon \left(1 - (1-\varepsilon)^{1/3}\right)^2}{36\beta \left[(1-\varepsilon)^{1/3} - (1-\beta\varepsilon)\right]} \tag{19}$$

4.4. Effective thermal conductivity models for high-porosity metal foams

Many investigations have been conducted to evaluate the effective thermal conductivity k_e as a key factor in the thermal analysis of such systems. Among them is the model established by Paek et al. [54] based on one-dimensional heat conduction through a cubic unit cell (Eq. (20)). This model indicates that foam porosity has a direct impact on the overall thermal conductivity unlike the pore size, which was found to have a marginal influence.

The theoretical model derived by Calmidi and Mahajan [58] for the effective thermal conductivity as a function of the foam porosity (Eq. (21)) was found to match well with the experiments for both air and water as fluid phase. Similarly, Bhattacharya et al. [52] examined a two-dimensional unit cell shaped as a hexagonal honey comb to estimate the effective thermal conductivity, but taking into account circular nodes at each intersection joint rather than the square nodes considered earlier by Calmidi and Mahajan [58]. Although this model showed excellent agreement with the experimental data obtained and its formulations detailed in Eq. (22) look mathematically simpler than that derived by Calmidi and Mahajan [58], it is in fact more complicated because this model is valid only for a limited case when the intersection size R approaches zero, which implies that $r \to \infty$.

A tetrakaidecahedron unit cell was adopted by Boomsma and Poulikakos [59] to estimate the effective thermal conductivity. Despite the fact that taking tetrakaidecahedron topology into account can provide a better estimation, it leads to more complex formulae, detailed in Eq. (23). Moreover, it was found that this model includes some aspects need to be adjusted as found by Dai et al. [60] (Eq. (24)). Based on the tetrakaidecahedron unit cell as well but with assuming one-dimensional heat conduction along the highly tortuous ligaments, a quite simplistic model (Eq. (25)) was recently derived by Yang et al. [61] for effective thermal conductivity of metal foams saturated with low conducting fluids, for example, air. However, this model is limited to highly conducting foams, where heat conduction is assumed to occur only along the tortuous ligaments ignoring the heat conduction through the fluid phase. More recently, the 3D tetrakaidecahedron unit cell was considered by Yao et al. [62] to establish a more realistic formulation for effective thermal conductivity (Eq. (26)) through taking into account the concavity and orientation of the tri-prism ligaments and for four pyramids nodes. In addition to including no empirical parameters, this model has outperformed, in terms of accuracy, what were reported earlier in the literature [62].

Paek et al. [54]:

$$k_e = k_f(1-t)^2 + k_s t^2 + \frac{2t(1-t)k_f k_s}{k_f t + k_s(1-t)}, \quad t = \frac{1}{2} + \cos\left(\frac{1}{3}\cos^{-1}(2\varepsilon - 1) + \frac{4\pi}{3}\right) \tag{20}$$

Calmidi and Mahajan [58]:

$$k_e = \left\{ \frac{2}{\sqrt{3}} \left[\frac{r\left(\frac{b}{L}\right)}{k_f + \left(1+\frac{b}{L}\right)\frac{\left(k_s - k_f\right)}{3}} + \frac{(1-r)\left(\frac{b}{L}\right)}{k_f + \frac{2}{3}\left(\frac{b}{L}\right)\left(k_s - k_f\right)} + \frac{\frac{\sqrt{3}}{2} - \frac{b}{L}}{k_f + \frac{4r}{3\sqrt{3}}\left(\frac{b}{L}\right)\left(k_s - k_f\right)} \right] \right\}^{-1}$$

$$\frac{b}{L} = \frac{-r + \sqrt{r^2 + \frac{2}{\sqrt{3}}(1-\varepsilon)\left[2 - r\left(1 + \frac{4}{\sqrt{3}}\right)\right]}}{\frac{2}{3}\left[2 - r\left(1 + \frac{4}{\sqrt{3}}\right)\right]}, \quad and, r = 0.09 \tag{21}$$

http://dx.doi.org/10.5772/intechopen.70451

Bhattacharya et al. [52]:

$$k_e = \left\{ \frac{2}{\sqrt{3}} \left[\frac{\frac{t}{L}}{k_f + \frac{(k_s - k_f)}{3}} + \frac{\frac{\sqrt{3}}{2} - \frac{t}{L}}{k_f} \right] \right\}^{-1}, \quad \frac{t}{L} = \frac{-\sqrt{3} - \sqrt{3 + (1-\varepsilon)(\sqrt{3}-5)}}{1 + \frac{1}{\sqrt{3}} - \frac{8}{3}} \tag{22}$$

Boomsma and Poulikakos [59]:

$$\left.\begin{aligned} k_e &= \frac{\sqrt{2}}{(R_A + R_B + R_C + R_D)} \\ R_A &= \frac{4d}{[2e^2 + \pi d(1-e)]k_s + [4 - 2e^2 - \pi d(1-e)]k_f} \\ R_B &= \frac{(e-2d)^2}{(e-2d)e^2 k_s + [2e - 4d - (e-2d)e^2]k_f} \\ R_C &= \frac{\left(\sqrt{2} - 2e\right)^2}{2\pi d^2\left(1 - 2e\sqrt{2}\right)k_s + 2\left[\sqrt{2} - 2e - \pi d^2\left(1 - 2e\sqrt{2}\right)\right]k_f} \\ R_D &= \frac{2e}{e^2 k_s + (4 - e^2)k_f} \\ d &= \sqrt{\frac{\sqrt{2}\left[2 - (5/8)e^3\sqrt{2} - 2\varepsilon\right]}{\pi\left(3 - 4e\sqrt{2} - e\right)}}, \text{and,} \quad e = 0.339 \end{aligned}\right\} \tag{23}$$

Dai et al. [60]:

$$\left.\begin{aligned} R_C &= \frac{\sqrt{2} - 2e}{\sqrt{2}\pi d^2 k_s + \left(2 - \sqrt{2}\pi d^2\right)k_f} \\ d &= \sqrt{\frac{\sqrt{2}\left[2 - (3/4)e^3\sqrt{2} - 2\varepsilon\right]}{\pi\left(3 - 2e\sqrt{2} - e\right)}}, \text{and,} \quad e = 0.198 \end{aligned}\right\} \tag{24}$$

Yang et al. [61]:

$$k_e = \frac{1}{3}(1-\varepsilon)k_s \tag{25}$$

Yao et al. [62]:

$$\left.\begin{aligned} k_e &= \frac{1}{(\lambda/k_A)+((1-2\lambda)/k_B)+(\lambda/k_C)} \\ k_A &= \frac{\sqrt{2}}{6}\pi\lambda(3-4\lambda)\frac{1+a_1^2}{a_1^2}k_s + \left[1-\frac{\sqrt{2}}{6}\pi\lambda(3-4\lambda)\frac{1+a_1^2}{a_1^2}\right]k_f \\ k_B &= \frac{\sqrt{2}}{2}\pi\lambda^2\frac{1+a_1^2}{a_1^2}k_s + \left(1-\sqrt{2}\pi\lambda^2\frac{1+a_1^2}{a_1^2}\right)k_f \\ k_C &= \frac{\sqrt{2}}{6}\pi\lambda^2\frac{1+a_1^2}{a_1^2}k_s + \left(1-\frac{\sqrt{2}}{6}\pi\lambda^2\frac{1+a_1^2}{a_1^2}\right)k_f \\ \varepsilon &= 1-\frac{\sqrt{2}}{2}\pi\lambda^2(3-5\lambda)\frac{1+a_1^2}{a_1^2}, \quad and, \quad a_1 = 2.01 \end{aligned}\right\} \tag{26}$$

4.5. Solid–fluid interstitial thermal exchange within open-cell metal foams

The condition of local thermal equilibrium (LTE) often occurs between the fluid and solid phases when a fluid flows across a permeable medium formed of comparably thermally conductive material. This makes the temperature difference between the two phases negligibly small. However, when the solid thermal conductivity is much higher than the corresponding value for the fluid phase, for example, metal foams, the assumption of LTE is no longer valid and usually results in an overestimation of the heat transported between the two phases. Hence, taking into account the local thermal nonequilibrium (LTNE) between the two phases becomes indispensable in metal foams, where two energy equations are coupled together to predict heat transfer in each phase separately.

Three principal heat transfer modes take place when a low conductive fluid flows across the ligaments of highly conductive foam: convection between the solid and fluid phases besides conduction via each one of the two phases. Thus, the three key parameters required for applying the LTNE approach are the effective thermal conductivity of the fluid k_{fe} and solid k_{se} phases in addition to the interstitial specific heat transfer rate between the two phases (a_{sf} h_{sf}), which depends on the foam structure and the flow regime across it.

The interstitial heat exchange rate depends on two individual quantities: the interfacial specific surface area a_{sf} and the solid-to-fluid interfacial heat transfer coefficient h_{sf}. By utilizing the dodecahedral structure of open-cell foams and taking into account the noncircular fiber cross section, the solid-to-fluid interfacial specific surface area a_{sf} was modeled by Calmidi and Mahajan [63] for arrays of cylinders that intersect in three mutually perpendicular directions (Eq. (27)), while Fourie and Du Plessis [49] established another model based on the cubic unit-cell representation (Eq. (28)). However, Schampheleire et al. [6] observed that the a_{sf} values estimated using Eq. (27) by Calmidi and Mahajan [63] deviates seriously from those obtained experimentally through a μCT scan with differences up to 233%, while the model of Fourie and Du Plessis [49] performs much better with up to 22% deviation from the experimental data of the full μCT scan.

Calmidi and Mahajan [63]:

$$a_{sf} = \frac{3\pi d_f}{\left(0.59 d_p\right)^2} \left[1 - e^{-(1-\varepsilon)/0.04}\right] \tag{27}$$

Fourie and Du Plessis [49]:

$$a_{sf} = \frac{3}{d}(3 - \chi)(\chi - 1) \tag{28}$$

With regard to estimating the solid–fluid interfacial heat transfer coefficient in high-porosity metal foams, Calmidi and Mahajan [63] proposed a correlation for interfacial Nusselt number as a function of both the foam porosity and fiber diameter (Eq. (29)). Another model was established by Shih et al. [28] for Nusselt number as a function of the foam porosity and pore diameter (Eq. (30)), where *a* and *b* are constants depending on the geometrical characteristics of the foam samples used in the experiments conducted. The correlations developed by Zukauskas [64] for staggered cylinders are widely used as a model to predict the interfacial Nusselt number as a function of the foam porosity, fiber diameter, and the value of Reynolds number (Eq. (31)), which makes it more general than the one proposed by Calmidi and Mahajan [63] as it is valid for a limited range of Reynolds numbers (40–1000).

Calmidi and Mahajan [63]:

$$Nu_{sf} = \frac{h_{sf} d_f}{k_f} = C_T \mathrm{Re}_{d_f}^{0.5} \mathrm{Pr}^{0.37} = 0.52 \sqrt{\frac{u d_f}{\varepsilon \upsilon}} \mathrm{Pr}^{0.37} \tag{29}$$

Shih et al. [28]:

$$Nu_{D_P} = \frac{h D_P}{k_{se}} = a \mathrm{Re}_{D_P}^{b} = a \left(\frac{\rho u D_P}{\mu}\right)^b \tag{30}$$

Zukauskas [64]:

$$Nu_{sf} = \frac{h_{sf} d}{k_f} = \left\{ \begin{array}{ll} 0.76 \mathrm{Re}_d^{0.4} \mathrm{Pr}^{0.37}, & (1 \le \mathrm{Re}_d \le 40) \\ 0.52 \mathrm{Re}_d^{0.5} \mathrm{Pr}^{0.37}, & \left(40 \le \mathrm{Re}_d \le 10^3\right) \\ 0.26 \mathrm{Re}_d^{0.6} \mathrm{Pr}^{0.37}, & \left(10^3 \le \mathrm{Re}_d \le 2 \times 10^5\right) \end{array} \right\} \tag{31}$$
$$d = \left(1 - e^{-(1-\varepsilon)/0.04}\right) \; d_f$$

Author details

Ahmed Niameh Mehdy Alhusseny[1,2]*, Adel Nasser[2] and Nabeel M J Al-zurfi[1]

*Address all correspondence to: ahmedn.alhusseini@uokufa.edu.iq

1 Mechanical Engineering Department, Faculty of Engineering, University of Kufa, Iraq

2 School of Mechanical, Aerospace and Civil Engineering, University of Manchester, UK

References

[1] Liu Z, Yao Y, Wu H. Numerical modeling for solid-liquid phase change phenomena in porous media: Shell-and-tube type latent heat thermal energy storage. Applied Energy. 2013;**112**:1222-1232

[2] Zhao CY. Review on thermal transport in high porosity cellular metal foams with open cells. International Journal of Heat and Mass Transfer. 2012;**55**:3618-3632

[3] Walz DD. Reticulated Foam Structure. Oakland: Energy Research & Generation Inc.; 1976

[4] ERG Materials & Aerospace. ERG Duocel® Foam [Internet]. Available from: http://www.ergaerospace.com/index.html [Accessed: 19-06-2017]

[5] MAYSER®. Foam Technology & Moulding [Internet]. Available from: http://www.mayser.com/en/foamtechnology-and-moulding [Accessed: 24-06-2017]

[6] De Schampheleire S, De Jaeger P, De Kerpel K, Ameel B, Huisseune H, De Paepe M. How to study thermal applications of open-cell metal foam: Experiments and computational fluid dynamics. Materials. 2016;**9**(2):1-27/94

[7] Alveotec. The Metal Foam by Alvéotec or Honeycomb Casting Process [Internet]. Available from: http://www.alveotec.fr/en/innovation.html [Accessed: 26-06-2017]

[8] Xu C, Mao Y, Hu Z. Tonal and broadband noise control of an axial flow fan with metal foams: Design and experimental validation. In: 22nd AIAA/CEAS Aeroacoustics Conference, Aeroacoustics Conferences, (AIAA 2016–3062); 30 May–1 June; Lyon, France. AIAA; 2016

[9] Dixit T, Ghosh I. Radiation heat transfer in high porosity open-cell metal foams for cryogenic applications. Applied Thermal Engineering. 2016;**102**:942-951

[10] Borovinšek M, Ren Z. Computational modelling of irregular open-cell foam behaviour under impact loading. Materials Science & Engineering Technology. 2008;**39**(2):114-120

[11] Boomsma K, Poulikakos D, Zwick F. Metal foams as compact high performance heat exchangers. Mechanics of Materials. 2003;**35**:1161-1176

[12] Mahjoob S, Vafai K. A synthesis of fluid and thermal transport models for metal foam heat exchangers. International Journal of Heat and Mass Transfer. 2008;**51**:3701-3711

[13] Ejlali A, Ejlali A, Hooman K, Gurgenci H. Application of high porosity metal foams as air-cooled heat exchangers to high heat load removal systems. International Communications in Heat and Mass Transfer. 2009;**36**:674-679

[14] Straatman AG, Gallego NC, Thompson BE, Hangan H. Thermal characterization of porous carbon foam-convection in parallel flow. International Journal of Heat and Mass Transfer. 2006;**49**:1991-1998

[15] T'Joen C, De Jaeger P, Huisseune H, Van Herzeele S, Vorst N, De Paepe M. Thermo-hydraulic study of a single row heat exchanger consisting of metal foam covered round tubes. International Journal of Heat and Mass Transfer. 2010;**53**:3262-3274

[16] Odabaee M, Hooman K. Metal foam heat exchangers for heat transfer augmentation from a tube bank. Applied Thermal Engineering. 2012;**36**:456-463

[17] Dai Z, Nawaz K, Park Y, Chen Q, Jacobi AM. A comparison of metal-foam heat exchangers to compact multi-louver designs for air-side heat transfer applications. Heat Transfer Engineering. 2012;**33**:21-30

[18] Huisseune H, De Schampheleire S, Ameel B, De Paepe M. Comparison of metal foam heat exchangers to a finned heat exchanger for low Reynolds number applications. International Journal of Heat and Mass Transfer. 2015;**89**:1-9

[19] Xu HJ, Qu ZG, Tao WQ. Numerical investigation on self-coupling heat transfer in a counter-flow double-pipe heat exchanger filled with metallic foams. Applied Thermal Engineering. 2014;**66**:43-54

[20] Chen X, Tavakkoli F, Vafai K. Analysis and characterization of metal foam-filled double-pipe heat exchangers. Numerical Heat Transfer, Part A: Applications. 2015;**68**:1031-1049

[21] Alhusseny A, Turan A, Nasser A, Al-zurfi N. Performance improvement of a counter-flowing double-pipe heat exchanger partially filled with a metal foam and rotating coaxially. In: 12th International Conference on Heat Transfer, Fluid Mechanics and Thermodynamics; 11–13 July; Costa del Sol, Malaga. 2016. pp. 1368-1377

[22] Alhusseny A, Turan A, Nasser A. Rotating metal foam structures for performance enhancement of double-pipe heat exchangers. International Journal of Heat and Mass Transfer. 2017;**105**:124-139

[23] Alhusseny A, Turan A. Effects of centrifugal buoyancy on developing convective laminar flow in a square channel occupied with a high porosity fibrous medium. International Journal of Heat and Mass Transfer. 2015;**82**:335-347

[24] Alhusseny A, Turan A, Nasser A, Hidri F. Hydrodynamically and thermally developing flow in a rectangular channel filled with a high porosity fiber and rotating about a parallel axis. International Communications in Heat and Mass Transfer. 2015;**67**:114-123

[25] Alhusseny A, Turan A, Nasser A. Developing convective flow in a square channel partially filled with a high porosity metal foam and rotating in a parallel-mode. International Journal of Heat and Mass Transfer. 2015;**90**:578-590

[26] Sleiti AK, Kapat JS. Heat transfer in channels in parallel-mode rotation at high rotation numbers. Journal of Thermophysics and Heat Transfer. 2006;**20**:748-753

[27] Kuo SM, Tien CL. Heat transfer augmentation in a foam-material filled duct with discrete heat sources. In: Intersociety Conference on IEEE Thermal Phenomena in the Fabrication and Operation of Electronic Components (I-THERM '88); 11–13 May. Los Angeles, CA. 1988. pp. 87-91

[28] Shih WH, Chiu WC, Hsieh WH. Height effect on heat-transfer characteristics of aluminium-foam heat sinks. Journal of Heat Transfer. 2006;**128**:530-537

[29] Bhattacharya A, Mahajan RL. Metal foam and finned metal foam heat sinks for electronics cooling in buoyancy-induced convection. Journal of Electronic Packaging. 2006;**128**: 259-266

[30] CT DG, Straatman AG, Betchen LJ. Modeling forced convection in finned metal foam heat sinks. Journal of Electronic Packaging. 2009;**131**:1-10/021001

[31] Kuang JJ, Kim T, Xu ML, Lu TJ. Ultralightweight compact heat sinks with metal foams under axial fan flow impingement. Heat Transfer Engineering. 2012;**33**(7):642-650

[32] Krishnan S, Hernon D, Hodes M, Mullins J, Lyons AM. Design of complex structured monolithic heat sinks for enhanced air cooling. IEEE Transactions on Components, Packaging and Manufacturing Technology. 2012;**2**(2):266-277

[33] Feng SS, Kuang JJ, Lu TJ, Ichimiya K. Heat transfer and pressure drop characteristics of finned metal foam heat sinks under uniform impinging flow. Journal of Electronic Packaging. 2015;**137**:1-12/021014

[34] Tzeng S-C, Soong C-Y, Wong S-C. Heat transfer in rotating channel with open cell porous aluminium foam. International Communications in Heat and Mass Transfer. 2004;**31**:261-272

[35] Jeng T-M, Tzeng S-C, Xu R. Experimental study of heat transfer characteristics in a 180-deg round turned channel with discrete aluminium-foam blocks. International Journal of Heat and Mass Transfer. 2014;**71**:133-141

[36] Azzi W, Roberts WL, Rabiei A. A study on pressure drop and heat transfer in open cell metal foams for jet engine applications. Materials & Design. 2007;**28**:569-574

[37] Williams LJ, Meadows J, Agrawal AK. Passive control of thermoacoustic instabilities in swirl stabilized combustion at elevated pressures. International Journal of Spray and Combustion Dynamics. 2016;**8**:173-182

[38] Zhao CY, Lu W, Tian Y. Heat transfer enhancement for thermal energy storage using metal foams embedded within phase change materials (PCMs). Solar Energy. 2010;**84**: 1402-1412

[39] Alhusseny A, Nasser A, Al-Fatlawi A. Metal foams as an effective means to improve the performance of PCM thermal storage systems. In: 7th International Symposium on Energy; 13–17 August. Manchester, UK; 2017

[40] Li WQ, Qu ZG, He YL, Tao WQ. Experimental and numerical studies on melting phase change heat transfer in open-cell metallic foams filled with paraffin. Applied Thermal Engineering. 2012;**37**:1-9

[41] Chen Z, Gao D, Shi J. Experimental and numerical study on melting of phase change materials in metal foams at pore scale. International Journal of Heat and Mass Transfer. 2014;**72**:646-655

[42] Yang J, Yang L, Xu C, Du X. Experimental study on enhancement of thermal energy storage with phase-change material. Applied Energy. 2016;**169**:164-176

[43] Zhao CY, Wu ZG. Heat transfer enhancement of high temperature thermal energy storage using metal foams and expanded graphite. Solar Energy Materials & Solar Cells. 2011;**95**:636-643

[44] Wu ZG, Zhao CY. Experimental investigations of porous materials in high temperature thermal energy storage systems. Solar Energy. 2011;**85**:1371-1380

[45] Yang J, Du X, Yang L, Yang Y. Numerical analysis on the thermal behaviour of high temperature latent heat thermal energy storage system. Solar Energy. 2013;**98**:543-552

[46] Xu S, Bourham M, Rabiei A. A novel ultra-light structure for radiation shielding. Materials and Design. 2010;**31**:2140-2146

[47] Chen S, Bourham M, Rabiei A. Novel light-weight materials for shielding gamma ray. Radiation Physics and Chemistry. 2014;**96**:27-37

[48] Chen S, Bourham M, Rabiei A. Neutrons attenuation on composite metal foams and hybrid open-cell al foam. Radiation Physics and Chemistry. 2015;**109**:27-39

[49] Fourie JG, Du Plessis JP. Pressure drop modelling in cellular metallic foams. Chemical Engineering Science. 2002;**57**:2781-2789

[50] Calmidi VV. Transport Phenomena in High Porosity Metal Foams [Thesis]. University of Colorado: UMI; 1998

[51] Du Plessis P, Montillet A, Comiti J, Legrand J. Pressure drop prediction for flow through high porosity metallic foams. Chemical Engineering Science. 1994;**49**:3545-3553

[52] Bhattacharya A, Calmidi VV, Mahajan RL. Thermophysical properties of high porosity metal foams. International Journal of Heat and Mass Transfer. 2002;**45**:1017-1031

[53] Yang X, Bai J, Lu T. A simplistic analytical model of permeability for open-cell metallic foams. Chinese Journal of Theoretical and Applied Mechanics. 2014;**46**:682-686

[54] Paek JW, Kang BH, Kim SY, Hyun JM. Effective thermal conductivity and permeability of aluminium foam materials. International Journal of Thermophysics. 2000;**21**(2):453-464

[55] Liu JF, Wu WT, Chiu WC, Hsieh WH. Measurement and correlation of friction characteristic of flow through foam matrixes. Experimental Thermal and Fluid Science. 2006;**30**:329-336

[56] Tadrist L, Miscevic M, Rahli O, Topin F. About the use of fibrous materials in compact heat exchangers. Experimental Thermal and Fluid Science. 2004;**28**:193-199

[57] Dukhan N. Correlations for the pressure drop for flow through metal foam. Experiments in Fluids. 2006;**41**:665-672

[58] Calmidi VV, Mahajan RL. The effective thermal conductivity of high porosity fibrous metal foams. Journal of Heat Transfer. 1999;**121**:466-471

[59] Boomsma K, Poulikakos D. On the effective thermal conductivity of a three- dimensionally structured fluid-saturated metal foam. International Journal of Heat and Mass Transfer. 2001;**44**:827-836

[60] Dai Z, Nawaz K, Park YG, Bock J, Jacobi AM. Correcting and extending the Boomsma–Poulikakos effective thermal conductivity model for three-dimensional, fluid-saturated metal foams. International Communications in Heat and Mass Transfer. 2010;**37**:575-580

[61] Yang XH, Kuang JJ, Lu TJ, Han FS, Kim T. A simplistic analytical unit cell based model for the effective thermal conductivity of high porosity open-cell metal foams. Journal of Physics D: Applied Physics. 2013;**46**:1-6/255302

[62] Yao Y, Wu H, Liu Z. A new prediction model for the effective thermal conductivity of high porosity open-cell metal foams. International Journal of Thermal Sciences. 2015;**97**:56-67

[63] Calmidi VV, Mahajan RL. Forced convection in high porosity metal foams. Journal of Heat Transfer. 2000;**122**:557-565

[64] Zukauskas AA. Convective heat transfer in cross-flow. In: Kakac S, Shah RK, Aung W, editors. Handbook of Single-Phase Convective Heat Transfer. New York: Wiley; 1987